Monthly Notices of the ROYAL ASTRONOMICAL SOCIETY

MNRAS **469,** S230–S237 (2017) doi:10.1093/mnras/stx1623
Advance Access publication 2017 June 30

The $^{34}S/^{32}S$ isotopic ratio measured in the dust of comet 67P/Churyumov–Gerasimenko by *Rosetta*/COSIMA

J. A. Paquette,[1]★ K. Hornung,[2] O. J. Stenzel,[1] J. Rynö,[3] J. Silen,[3] J. Kissel,[1] M. Hilchenbach[1] and The Cosima Team

[1]*Max-Planck-Institut für Sonnensystemforschung, Justus-von-Liebig-Weg 3, D-37077 Göttingen, Germany*
[2]*Universität der Bundeswehr München, LRT 7, D-85577 Neubiberg, Germany*
[3]*Finnish Meteorological Institute, Observation services, Erik Palménin aukio 1, FI-00560 Helsinki, Finland*

Accepted 2017 June 23. Received 2017 June 23; in original form 2017 April 7

ABSTRACT

The isotopic ratio $^{34}S/^{32}S$ has been measured in cometary gas for a few comets, but it has only been measured in cometary dust by STARDUST. The dust measurements find a value of the ratio that is consistent with the Vienna Canyon Diablo Troilite value of 0.0442 within errors, but there is more spread in the values from cometary gas. In this paper, we present the result of measurements of the sulphur isotopic ratio in dust from Comet 67P/Churyumov–Gerasimenko with the COSIMA instrument aboard the *Rosetta* spacecraft. We find a result of 0.0463 ± 0.0057, which is consistent within errors with the terrestrial value.

Key words: comets: general – comets: individual: 67P/Churyumov–Gerasimenko.

1 INTRODUCTION

Cometary nuclei are thought to contain some of the most primitive materials in the Solar system both because the abundances of rock-forming elements match the Solar system values and because of the observed diversity of gas phase composition (Bockelée-Morvan et al. 2015). The STARDUST results showed that cometary dust from comet Wild 2 also contained objects resembling chondrules (Nakamura et al. 2008; Nakashima et al. 2012; Ogliore et al. 2012) and calcium–aluminium-rich inclusions (McKeegan et al. 2006; Simon et al. 2008; Joswiak, Brownlee & Matrajt 2013), which were presumably produced close to the proto-sun under high-temperature conditions. Compositional evidence for calcium–aluminium-rich inclusions has also been seen in the dust of comet 67P/Churyumov–Gerasimenko (hereafter 67P; Paquette et al. 2016). Thus, cometary matter is therefore a mixture of components with different origins. Isotopic composition can give important information about a material's history, since isotopic fractionation is sensitive to conditions such as density, temperature and radiation. In this work, we will consider the isotopic abundance of sulphur, the tenth most abundant element in the universe.

The first sulphur-bearing species detected in a comet was CS, observed in C/1975 West (Smith, Stecher & Casswell 1980). Since then many other such species have been detected. For example, SO, SO_2, OCS, CS_2, H_2S, S_2, S_3, S_4, CH_3SH, H_2CS, NS and C_2H_6S have all been observed in cometary gas (Canaves et al. 2007; Calmonte et al. 2016). The isotopic ratio $^{34}S/^{32}S$ has been measured a few times in some of these species. Altwegg (1996) detected positive sulphur ions using *in situ* mass spectrometry to determine the sulphur isotopic ratio for comet 1P/Halley. Jewitt et al. (1997) used millimetre spectroscopy to quantify CS for comet C/1995 O1 (Hale–Bopp) and Biver et al. (2008) used the same technique for comet 17P/Holmes, and Biver et al. (2016) did likewise for comets C/2012 F6 (Lemmon) and C/2014 Q2 (Lovejoy). Crovisier et al. (2004) measured H_2S for comet C/1995 O1. All of their results agree within 2σ with the Vienna Canyon Diablo Troilite (hereafter V-DCT) value of 0.0442, which serves as a terrestrial standard (Ding et al. 2001). The earlier results are summarized in the review by Bockelée-Morvan et al. (2015).

The measurements of the sulphur isotopic ratio in cometary dust are both the products of the STARDUST mission to comet 81P/Wild 2. Heck, Hoppe & Huth (2012) measured sulphur isotopic ratios in residues of impact craters on STARDUST aluminium foils. Nguyen et al. (2015) measured the ratio in cosmic symplectite, a material which consists of aggregates of nanocrystalline iron sulphides and magnetite (Nittler et al. 2015).

Recent work on comet 67P (Calmonte 2015) with the ROSINA instrument shows some variation in the $^{34}S/^{32}S$ isotopic ratio by the host species of the sulphur (H_2S, SO_2, CS_2, OCS and S_2), with depletions ranging from 5 per cent for H_2S to 36 per cent in gaseous S_2. The discrepancy between the ROSINA results and the STARDUST results is of interest. Is it due to a difference in isotopic composition between comets Wild 2 and Churyumov–Gerasimenko or is it indicative of a difference between sulphur isotopic ratios measured in cometary dust with those measured in cometary gas?

This work concerns the measurement of the $^{34}S/^{32}S$ ratio in cometary dust from Comet 67P. These measurements were made *in situ* using COSIMA (the COmetary Secondary Ion Mass Analyser) aboard the *Rosetta* orbiter. While measurement of $^{33}S/^{32}S$

★ E-mail: paquette@mps.mpg.de

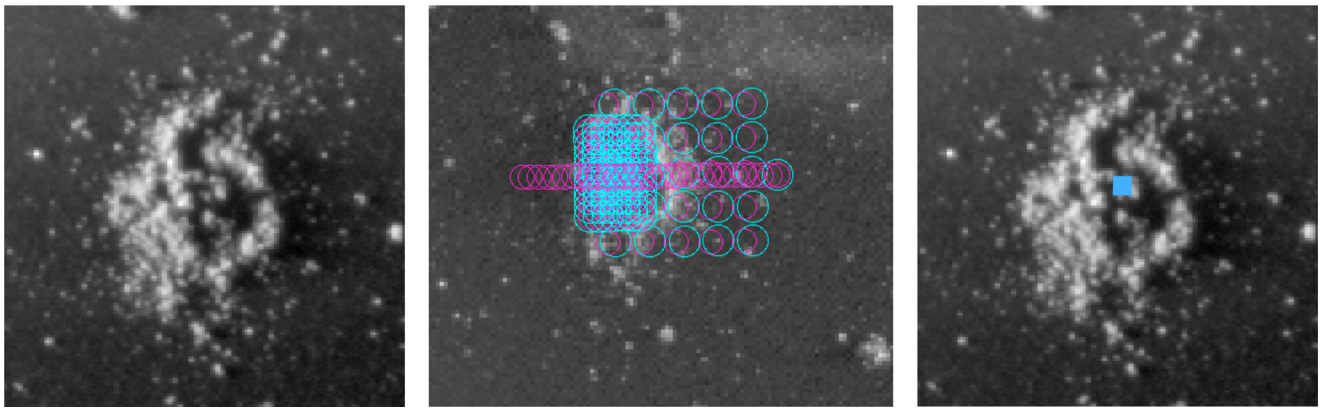

Figure 1. Images of the dust particle Jessica Lummene.2 on COSIMA Target 2CF. Panel (a) (from Langevin et al. 2016) shows a Nyquist sampled optical image of the particle which is about 550 × 650 μm across and 40 μ high. Jessica is considered to be a crossover between the shattered cluster and rubble pile categories (Langevin et al. 2016). Panel (b) shows the positive (magenta circles) and negative (cyan circles) spectra taken on Jessica prior to 2016 April. The centre of each circle shows the approximate location of the centre of the ion beam. Panel (c) depicts four locations (the four corners of the blue square) that were chosen for the very long measurement used to determine the sulphur isotopic ratio.

ratio would also be of interest, it is not possible to do so directly because of the strong interference at mass 33 from ^{32}SH. The mass of $^{33}S^-$ is 32.972 and that of $^{32}SH^-$ is 32.980, so the difference is too small to be resolved with COSIMA (mass resolution of ∼1400 at mass 100). By contrast, the interference from $^{33}SH^-$ at 33.980 is expected to be negligible. Comparison of the $^{33}SH^-$ peak and the $^{32}S^-$ peak suggest that sulphur hydride has an intensity about 20 times lower than the corresponding sulphur peak. This coupled with the low abundance of ^{33}S leads to an estimated contribution from $^{33}SH^-$ to the peak at mass 34, which is less than 1 per cent of the contribution from $^{34}S^-$. Any contribution from H_2O_2 at mass 34.006 can be easily resolved.

2 THE COSIMA INSTRUMENT

COSIMA was an instrument aboard the *Rosetta* spacecraft which was designed to capture, image and measure the composition of cometary dust particles. 24 target holders, each with 3 targets (1 cm × 1 cm in size), were kept in storage when not in use. Targets were covered with blacks from gold, silver, palladium or platinum. The targets used in this work were coated with gold black. This substance was formed by the evaporation of gold in a low-pressure argon atmosphere (Hornung et al. 2014). A target manipulator unit (TMU) moved a target holder in front of a dust funnel so that cometary dust entering the instrument could strike the target and adhere to it. The TMU could then move the target holder in front of COSISCOPE (an internal microscope camera) to be imaged, and then into the path of a beam of 8 keV $^{115}In^+$ ions for time-of-flight secondary ion mass spectrometry (ToF-SIMS). The primary indium ions eject secondary ions from dust particles on the target, which are directed into a reflectron for mass spectrometry. Precise measurement of the time of flight allows a precise measurement of the mass per charge of secondary ions. Since most such ions carry one unit of electric charge, this technique often directly yields the mass of the secondary ions. Thus, a mass spectrum of secondary ions is produced, providing composition information on a cometary dust particle. The polarity can be set to collect secondary ions that are either positively or negatively charged. A more complete description of COSIMA is available in Kissel et al. (2007).

Previous missions to comets (such as STARDUST and Giotto) were flybys, spending a relatively short time close to the nucleus and having a large relative velocity of measured dust particles. Rosetta remained within tens to hundreds of kilometres of the nucleus of 67P for 2 yr, thus the relative velocity of arriving cometary dust particles was low – of the order of meters per second (Rotundi et al. 2015). Therefore, the particles collected by COSIMA are relatively unaltered in composition (apart from the loss of volatiles; since the temperature of COSIMA is 10°C–15°C, ices not lost during the passage from the comet to the orbiter will not long endure after collection) (Hilchenbach et al. 2016).

3 MEASUREMENT TECHNIQUE

One of the thousands of cometary dust particles collected on COSIMA targets is Jessica.Lummene.2, shown in Fig. 1. Jessica is a large particle (about 550 μm × 650 μm and 40 μm high) on COSIMA target 2CF. Jessica was collected in 2015 between January 26 04:57:02 and January 27 04:12:37. The median distance to the centre of the nucleus of 67P was 27.65 km. *Rosetta* was in a terminator orbit at the time of collection, the latitude range during the collection period was from −47.7° to +40.4°, and local standard time of the spacecraft pointing direction ranged from 12:33:58 to 20:52:56. Since this was well before the equinox, Jessica most probably came from the Northern hemisphere of the comet.

A technique called non-negative matrix factorization (Gillis & Vavasis 2014) was used on a set of spectra taken on and around Jessica. These spectra naturally contained a contribution from both the particle and the target, and NMF decomposed them into two components. One component was identified as being largely due to the target, the other as being largely cometary. Four locations (the corners of the blue box in Fig. 1c) were selected to minimize the contribution from the target substrate (and thus to maximize the cometary contribution). A long measurement was undertaken on the particle Jessica at these four locations. This measurement lasted almost 48 h, consisted of 2352 2.5-min spectra and resulted in over 7000 counts for ^{34}S. Data from this long Jessica measurement were used to compute the $^{34}S/^{32}S$ ratio. The isotopic ratio was also computed using spectra from three additional particles, but the analysis of Jessica will serve as an example of the techniques used.

It is necessary to account for interferences from other species at masses 32 and 34. To determine what species must be accounted for a correlation between selected masses was performed for the

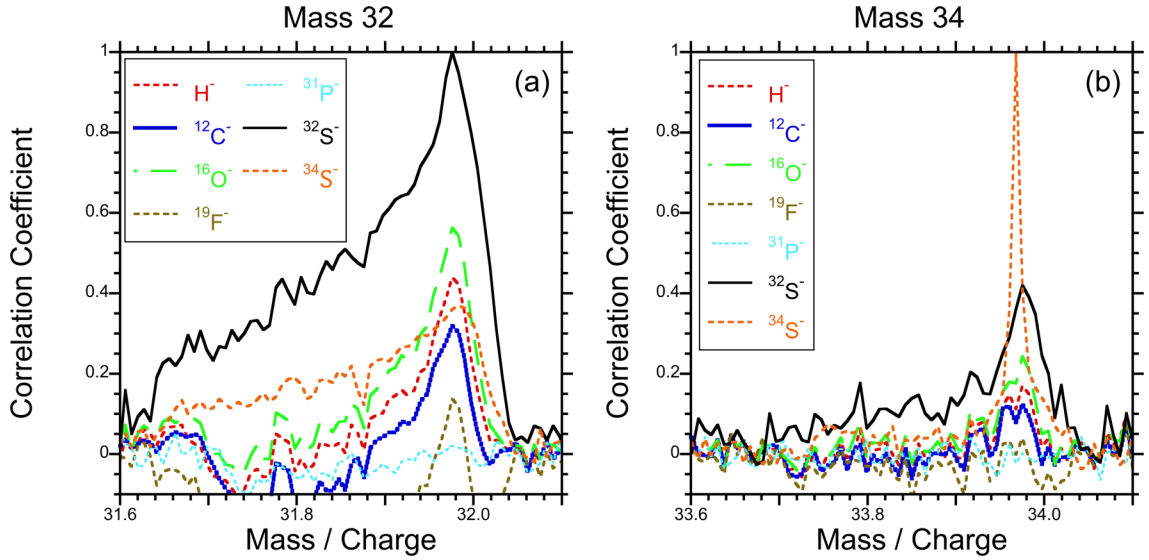

Figure 2. Sections of the correlation function between the mass spectrum and selected masses (corresponding to negative ions of H, C, O, F, P and S). Panel (a) shows the region near mass 32 and panel (b) shows the region near mass 34. Panel (a) shows that ^{32}S is the major constituent of the peak at mass 32, with some additional contribution from O_2. The weaker correlations with carbon, hydrogen, nitrogen and fluorine are due to target contamination. The lack of correlation with phosphorus indicates the absence of interference at this mass from PH^-. Panel (b) shows the expected correlation between the two S isotopes as well a weaker correlation with O and H (which may indicate the presence of $O_2H_2^-$) although the correlations are lower than at mass 32. Any N-bearing compounds would lie well to the right of the S, and thus will not interfere with it. The other correlations are due to contamination on the target substrate.

spectra resulting from the long measurement on Jessica. Two sections from the resulting correlation function are shown in Fig. 2. Fig. 2a shows the correlations with masses corresponding to negative ions of hydrogen, carbon, oxygen, fluorine, phosphorus and ^{32}S for the region near mass 32. Clearly, the entire peak at mass 32 (including its left tail, which is discussed below) is correlated with mass 31.973 at which $^{32}S^-$ is expected, indicating that sulphur is the major constituent of the peak. The correlation with oxygen indicates the presence of O_2^-, but at a lower level. The weaker correlations with hydrogen and fluorine are due to a small contribution from contaminants on the target substrate, which will have to be accounted for. The lack of correlation with phosphorus is evidence of the absence of any interference from PH^-.

Fig. 2b shows the correlations with masses corresponding to negative ions of H, C, N, O, F, P, ^{32}S and ^{34}S for the region near mass 34. The expected correlation between $^{34}S^-$ and $^{32}S^-$ is readily visible, and the correlation with oxygen and hydrogen may be indicative of the presence of $O_2H_2^-$ at a low level. The other, lower, correlations are due to target contamination, as above.

Sections from the spectrum resulting from the long measurement on Jessica are shown in Fig. 3. Panels a, b and c show regions of mass per charge near masses 32, 33 and 34, respectively. The left tail visible in all three panels is characteristic of COSIMA spectra in negative mode, when the ion beam is on a dust particle. The peak shape is probably the result of the dust being insulating, which may lead to a reduction of the apparent extraction voltage due to charging of the particle by the ion beam or due to particle height. The peak shape is useful as an indicator that the beam is in fact striking a particle (not merely the substrate). In the Jessica spectrum, this effect is particularly strong. Most peaks in the spectrum show this characteristic shape, but mass 197 (gold), which originates purely from the gold substrate, does not show the left tail.

The correlation results above and the location in mass of the peak at mass 32 indicate that it originates in $^{32}S^-$, likely with a contribution from O_2^-. The masses of these two species are shown as vertical lines on Fig. 3a. The peak at mass 33 probably contains some $^{33}S^-$, but since ^{33}S is much less abundant than ^{32}S and this peak has almost 60 per cent of the amplitude of the mass 32 peak, it is overwhelmingly dominated by $^{32}SH^-$. This unfortunately precludes a measurement of the $^{33}S/^{32}S$ ratio. In Fig. 3b, vertical lines show the mass of these two species. The peak at mass 34 is almost entirely due to ^{34}S, as both the peak mass and the correlation data indicate. While $O_2H_2^-$ is possible, Fig. 3c clearly shows that any such contribution must be very small indeed. The absence of a visible peak implies that the contribution of $O_2H_2^-$ to the observed counts can be no more than about 1 per cent. H_2S is expected to be a cation, so it will not be an interference in negative spectra. Of course, ^{33}SH must also be present, but only at a negligible level, as discussed above.

Normally, positive mode COSIMA spectra can be fitted by a Gaussian or by the sum of two or three Gaussians. Because of the unusual peak shape in negative mode, the fitting methods usually used for positive mode spectra had to be modified. The peak shape at mass 34 was used as a template to fit the peak at mass 32. Before this could be done, it was necessary to subtract a baseline level due to chemical noise, i.e. to the breakup of molecular ions during the process of acceleration (e.g. Cotter 1997). The rationale being that the peak at mass 34 consists almost solely of ^{34}S, so that it gives a clear picture of the peak shape for sulphur isotopes. While the peaks at both 32 and 34 result in part from contamination, which could in principle lead to some difference in peak shape if the isotopic ratio of the contamination and the cometary data are different, for Jessica the contribution from the target substrate 2CF is small enough that this has no practical effect. The width of this peak template was decreased slightly. The peak width in COSIMA is a function of time of flight, and an empirical curve derived from spectra measured in our reference model indicated a decrease by a factor of 0.991. Two mass peaks were allowed at mass 32 and their amplitude was allowed to vary freely. Their initial locations in time of flight were chosen to correspond to the masses of ^{32}S and O_2, with variation possible within a limited range (±1.5 time of flight

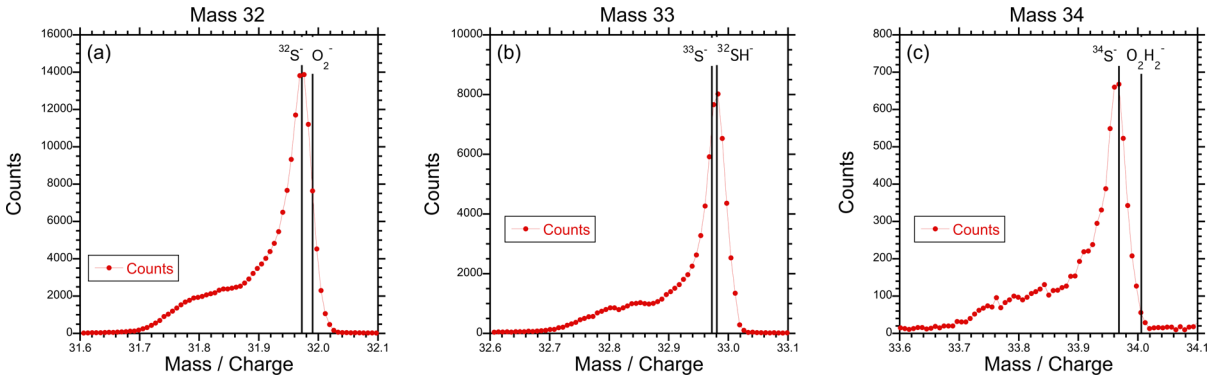

Figure 3. Sections from the spectrum resulting from a long measurement on Jessica. Panels a, b and c show regions of mass per charge near masses 32, 33 and 34, respectively. The left tail visible in all three panels is characteristic of COSIMA spectra in negative mode, when the ion beam is on a dust particle. In the Jessica spectrum, this effect is particularly strong. The vertical lines show the masses of $^{32}S^-$ and O_2^- in panel (a), $^{33}S^-$ and $^{32}SH^-$ in panel (b) and $^{34}S^-$ and $O_2H_2^-$ in panel (c).

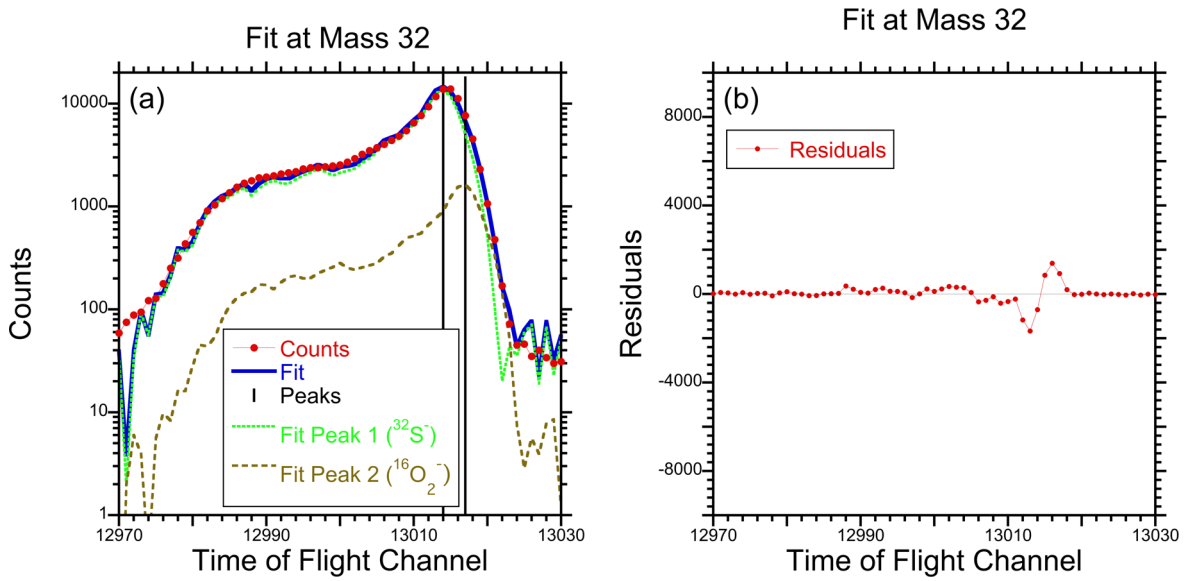

Figure 4. Results of fitting the peak at mass 32 using the shape of the peak at mass 34. Panel (a) shows the counts (red points), total fit function (blue solid line) and the two components of the fit corresponding to ^{32}S (green dotted line) and O_2 (brown dashed line). The vertical lines correspond to the locations selected by fitting and correspond to masses 31.978 and 31.995. Panel (b) shows the residuals left after the fit. The amplitude of these residuals is less than 10 per cent of the amplitude of the fit or counts, and the sum of the residuals is less than 0.2 per cent of the integral of the ^{32}S peak.

channels, roughly corresponding to ±0.007 amu). No baseline was used in the fit, as it was not needed. The results of this fit are shown in Fig. 4. The total counts of O_2 were about 12 per cent of the total counts of ^{32}S. Fig. 4b shows the residuals left after the fit. The amplitude of these residuals is less than 10 per cent of the amplitude of the fit or counts, and the sum of the residuals is less than 0.2 per cent of the integral of the ^{32}S peak.

The ratio is then formed between the integrated counts for ^{34}S and ^{32}S. The raw value of this ratio is 0.0478, but the contribution from the target must also be accounted for. While the locations chosen for the measurements on Jessica were selected to minimize target contribution, the effects of the target cannot be totally eliminated as the COSIMA ion beam spot is large, the particles are porous, and the SIMS efficiency of the target is higher than that of the particles. Thus, some of the counts seen at masses 32 and 34 were actually due to contamination (from compounds of terrestrial origin) on the target and to some degree on the particle itself, rather than from the cometary particle. Because of the long delay between collection and SIMS (about 15 months) some contaminants migrated from the target to the particle. To account for the target contribution, a spectrum resulting from measurements on target 2CF was also fit. The spectra used to characterize target 2CF were taken immediately before the spectra on Jessica, at a location about 4.4 mm away and not near any other dust particle. Sections from this spectrum near masses 32 and 34 are shown in Fig. 5. The left shoulder visible in the Jessica spectrum is absent as these spectra result solely from the target. The smaller satellite peak to the left of the main peak results from secondary electrons ejected by ions striking the entrance grid to the microsphere plate detector (Kissel et al. 2007), which (in negative mode, as here) are then accelerated to the detector.

To correct the measured value for ^{32}S for the contribution from the target, the target counts are normalized to the fragment of PDMS (polydimethylsiloxane) at mass 75, and the normalized target value is subtracted from the measured value from Jessica, thus

$$^{32}S_{\rm net} = {}^{32}S_{\rm particles} - {}^{32}S_{\rm target} \times \left(\frac{^{75}{\rm PDMS}_{\rm particles}}{^{75}{\rm PDMS}_{\rm target}} \right) \quad (1)$$

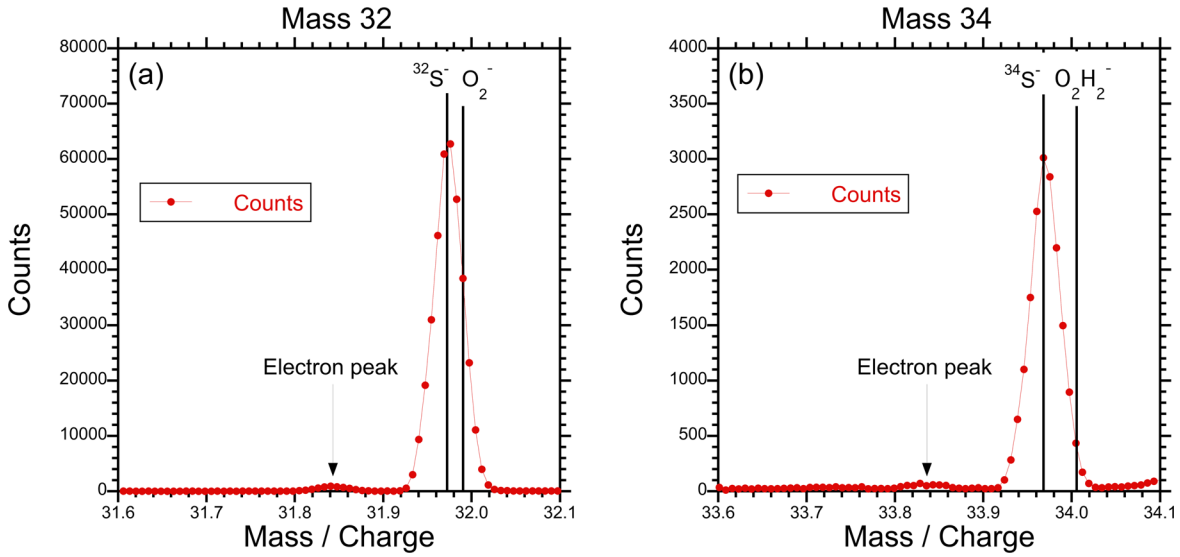

Figure 5. Sections from a spectrum taken on target 2CF near masses 32 (panel a) and 34 (panel b). The points indicate data and the vertical lines indicate the masses of the labelled species for comparison (they are not the results of fitting). The left shoulder visible in the Jessica spectrum is absent as these spectra result solely from the target, not from any cometary particle. The smaller satellite peak to the left of the main peak results from secondary electrons ejected by ions striking the entrance grid to the microsphere plate detector (Kissel et al. 2007).

The same technique was used to derive the net value of ^{34}S. PDMS is a contaminant on some COSIMA targets, the result of outgassing from wire insulation and other plastics. This technique eliminates a number of hydrocarbon peaks visible in positive mode, showing that they are not of cometary origin but rather due to target contamination.

In principle, instrumental mass fractionation (IMF) must be accounted for. In ToF-SIMS the heavier isotope can be slightly less efficiently ionized than the lighter isotope. Bullock et al. (2010) saw IMF values ranging from −2.18 ‰ to +2.68 ‰, depending on sample material. To evaluate the effect of IMF, terrestrial sulphur samples were examined in the COSIMA reference model (RM) on targets 0514 and 0516. These data indicate that IMF is too small to be measureable for the ^{34}S/^{32}S ratio in COSIMA, as there are simply insufficient statistics.

To estimate the uncertainty in the isotopic ratio, the 1σ statistical errors based on counting statistics (about 1.2 per cent) were combined in quadrature with the systematic errors. The systematic errors include a term from the correction based on subtraction of the normalized target, but the larger term comes from uncertainty in the fitting. It is possible to achieve equally good fits (i.e. fits with equally low residuals) in more than one way. The ^{34}S/^{32}S ratio resulting from each such fit was computed, and half the difference between the highest and lowest values was used as an estimate of the error resulting from fitting. This was the largest contribution to the uncertainty. The resulting error (both statistical and systematic) is about 11 per cent.

In view of the observations by ROSINA of S_2, S_3 and S_4 (Calmonte et al. 2016), the latter two species being attributed to the dust, the mass peaks at 64, 96, 128 and 256 in the set of spectra from Jessica were checked for their degree of correlation with sulphur (and other species) as shown in Fig. 6. While S_8 has not been observed by ROSINA, it is the most common terrestrial form and was considered as a potential parent molecule for S_3 and S_4. The presence of S_3 and S_4 might allow fitting and comparison at these higher masses as a useful cross-check on the isotopic ratio determined from masses 32 and 34. However, while Fig. 6 shows a hint of the presence of ^{32}S in the mass 64 peak and in the mass 96 peak, there is no such hint at mass 128 or mass 256. Fitting (using the appropriately scaled mass 34 peak as a template as described above) indicates that the sulphur contributing to the mass 64 peak consists of both S_2 and SO_2, with the latter being dominant. Similarly, fitting indicates that the weak sulphur correlation seen at mass 96 consists of both S_3 and SO_4. In both cases, at least one additional organic contaminant is also present – probably $CH_4O_3^-$ at mass 64 and possibly $C_4H_4N_2O^-$ at mass 96. SO_2 or SO_4 could be contamination rather than cometary. Broadly speaking, isotopic ratios derived from the fits to masses 64 and 66 agree with the results derived from 32 and 34, but the low statistics involved limit the accuracy of such a determination.

While neither S_4 nor S_8 was observed on the dust particle Jessica, measurements on S_8 using the COSIMA RM indicate that the instrument efficiency for S_4 is low and the efficiency for S_8 is extremely low. Thus, the lack of observation could be due to instrumental bias.

The measurement technique on Jessica was then repeated on three more cometary dust particles collected by COSIMA: Kerttu Rikkavesi on target 3D0, Andrzej Ukonvesi on target 1D0 and Günter Jerisjarvi.1 on target 1D2.

4 RESULTS

The average ^{34}S/^{32}S ratio measured for four cometary particles is 0.0463 ± 0.0057, where the error here is simply the standard deviation of the four values. For the sake of comparison, the target value of the isotopic ratio was 0.049 ± 0.0033. Counts resulting from the target contributed from 10 per cent to 50 per cent of the measured counts. The results of the individual measurements on the dust are shown in Table 1. The ratios measured in the four COSIMA dust particles (which, collectively, have an estimated mass of 7 μg) are compared to the V-CDT standard and to other values measured in comets in Fig. 7. Fig. 7a shows a series of measurements of the sulphur isotopic ratio in cometary gas (taken from Bockelée-Morvan et al. 2015; Biver et al. 2016; Calmonte 2015), results from

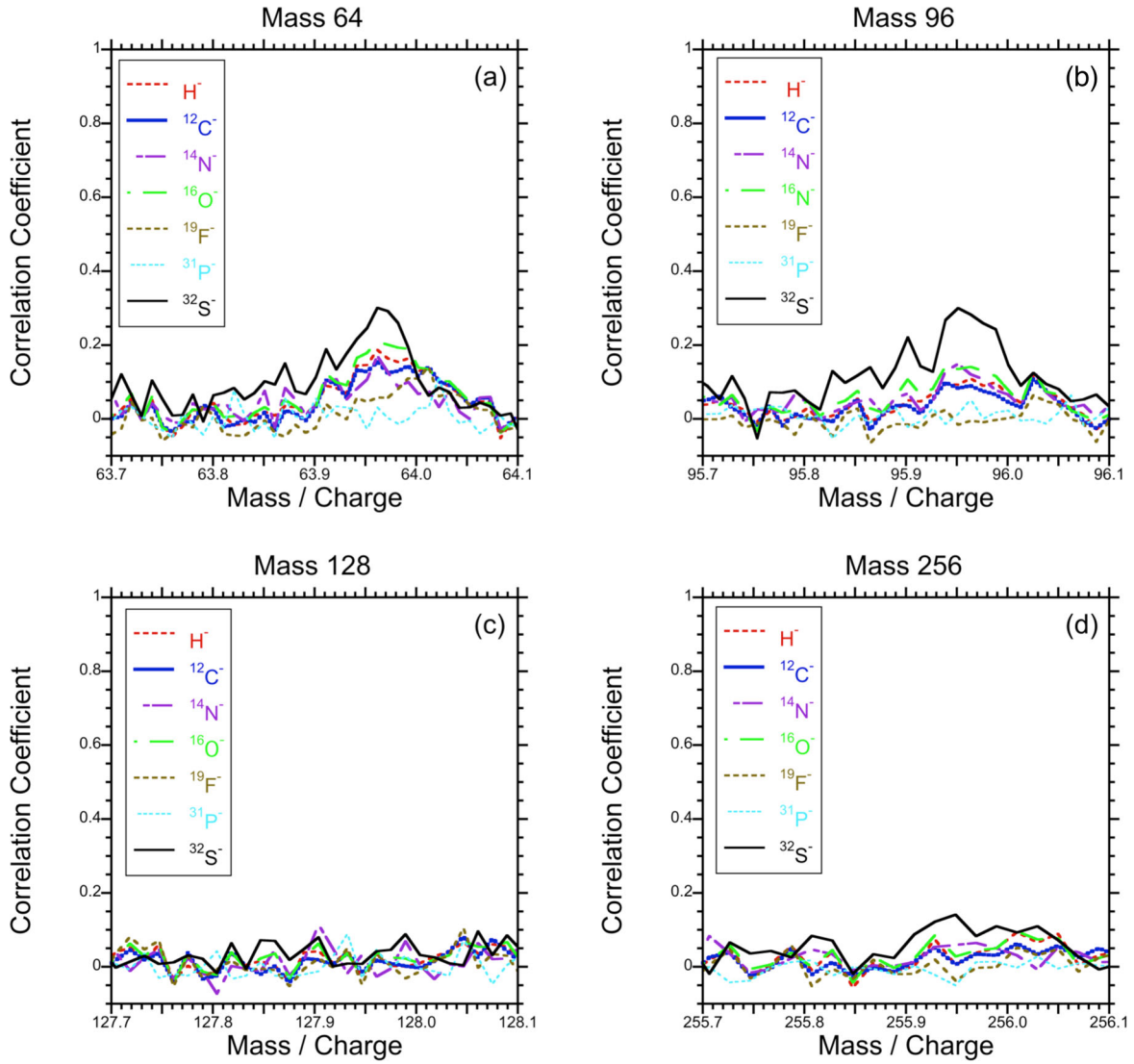

Figure 6. Sections of the correlation function between the mass spectrum and selected masses (corresponding to negative ions of H, C, N, O, F, P and S) near masses 64, 96, 128 and 256 (panels a, b, c and d, respectively). While there is a weak correlation for sulphur at masses 64 and 96, it is absent at masses 128 and 256. There is no evidence for the presence of S_4 or S_8 on the particle Jessica.

Table 1. Dust particles for which the sulphur isotopic ratio has been measured, their COSIMA target, collection time, and the ratio itself. The average ratio for all 4 particles is also shown.

Dust particle	Target	Collection date and time	$^{34}S/^{32}S$
Jessica.Lummene.2	2CF	2015-01-26 04:57:02 – 2015-01-27 04:12:37	$0.0488 \pm 5.4 \times 10^{-3}$
Kerttu Rikkavesi	3D0	2014-10-18 04:03:04 – 2014-10-24 18:49:11	$0.0384 \pm 4.7 \times 10^{-3}$
Andrzej Ukonvesi	1D0	2014-11-07 17:44:07 – 2014-11-14 07:09:12	$0.0463 \pm 5.2 \times 10^{-3}$
Günter Jerisjarvi.1	1D2	2016-02-29 14:54:29 – 2016-03-01 09:00:28	$0.0516 \pm 6.9 \times 10^{-3}$
Average of four particles	–	–	$0.0463 \pm 5.7 \times 10^{-3}$

STARDUST samples (Heck et al. 2012; Nguyen et al. 2015) and the results of this work.

The isotopic ratio for 1P/Halley was measured in S^+ (Altwegg 1996). The ratio was measured in CS by Jewitt et al. (1997) for C/1995 O1 and by Biver et al. (2008) for comet 17P/Holmes. Crovisier et al. (2004) determined the ratio in H_2S for comet C/1995 O1. Biver et al. (2016) measured the sulphur isotopic ratio in CS for C/2012 F6 and C/2014 Q2. Calmonte (2015) measured the isotopic ratio in H_2S, SO_2, CS_2, OCS and S_2, and these measured ratios are represented in that order by five points in Fig. 7. Heck et al. (2012) measured the ratio in dust impact residues taken from craters on the STARDUST aluminium foils. The value plotted in Fig. 7a (and in 7b) are an average of the 24 samples that were measured, and the error bar is the sample standard deviation (both taken from table 2 of Heck et al. 2012). Nguyen et al. (2015) measured the sulphur isotopic ratio in a terminal particle from STARDUST track #147, which was identified as cosmic symplectite of pentlandite and nanocrystalline maghemite with high calcium pyroxene.

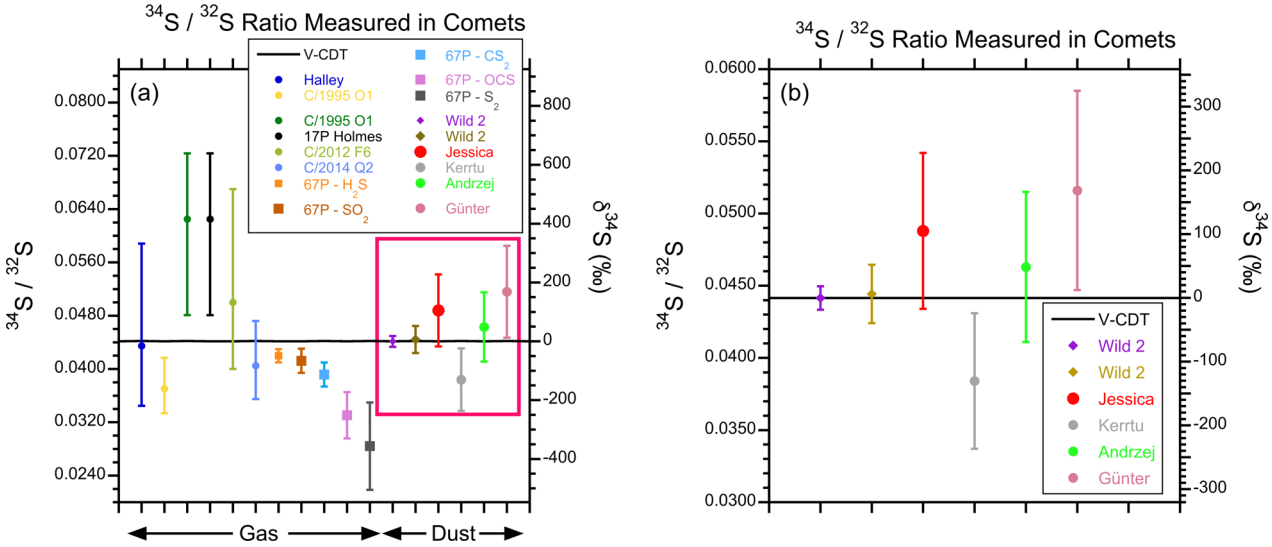

Figure 7. Comparison of results from this work with other values of the sulphur isotopic ratio with the V-CDT value shown for reference. Panel (a) shows a series of measurements of the sulphur isotopic ratio (taken from Bockelée-Morvan et al. 2015 and Biver et al. 2016), and five results from different gaseous species using ROSINA (Calmonte 2015), as well as results from residues taken from impact craters on the STARDUST aluminium foils (Heck et al. 2012), from a terminal particle from STARDUST track #147 (Nguyen et al. 2015) and the results of this work. Results measured in cometary gas are to the left, and results measured in cometary dust are to the right, with the results of this work plotted to the extreme right. The red box in panel (a) shows the region which is plotted on a larger scale in panel (b), which includes only measurements from dust. The COSIMA result agrees within errors with the V-DCT value and with the STARDUST values.

The maroon box in Fig. 7a shows the region which is plotted at larger scale in Fig. 7b. Only isotopic measurements of the dust are included in Fig. 7b. Except for the result from particle Kerttu, the COSIMA results agree within errors with the terrestrial value and with the STARDUST values.

5 DISCUSSION

The variation of the sulphur isotopic composition in interplanetary dust particles and meteorites is relatively small (Mumma & Charnley 2011). Bullock et al. (2010) found δ^{34}S values ranging from −0.7 to 6.8 ‰ in CI1 chondrites, from −2.9 to 1.8 ‰ in CM1 chondrites and from −7.0 to 6.8 ‰ in CM2 chondrites. They attribute enhancement of the heavier isotope to the concentration of isotopically lighter sulphur in sulphates formed during aqueous alteration. Cooper et al. (1997) saw an enhancement of 11.27 per cent in methyl sulfonic acid from the Murchison meteorite. Defouilloy et al. (2016) found average δ^{34}S values below the per mille level for 24 enstatite chondrites of varying type. They found δ^{34}S ranging from −1.34 per cent to 0.154 per cent for aubrites. Gao & Thiemens (1993) saw variations below the per cent level in sulphates, sulphides and elemental sulphur in chondrites. Rai, Jackson & Thiemens (2005) and Farquhar, Jackson & Thiemens (2000) saw an even smaller variation in achondrites and ureilites. Mass independent fractionation is weaker still, below the per mille level (Labidi et al. 2017). In comets, a much greater variability seems to be present in the volatiles, but isotopic composition of cometary dust seems more consistent than that of cometary gas. The ^{34}S/^{32}S ratio measured in four COSIMA particles is in agreement with STARDUST results from impact residues in aluminium foil craters and from a terminal particle.

We cannot determine what compound or compounds is the source of the sulphur that we measured with COSIMA. It could be mineral or organic or a mixture. Fray et al. (2016) observed refractory organic matter in dust from 67P, and Cooper et al. (1997) reported organic sulfonic acids in the Murchison meteorite.

The differing values observed in cometary gas make for an interesting comparison. Mumma & Charnley (2011) suggest that confirmation of the enrichment seen by Croivisier et al. (2004) in H_2S would be of interest, as it is much greater than the compositional variation seen in primitive matter in carbonaceous chondrites and interplanetary dust particles (Busemann et al. 2006; Floss et al. 2006). However, the ROSINA measurement of the ^{34}S/^{32}S ratio in H_2S shows a depletion rather than an enhancement (Calmonte 2015). But variations from comet to comet in other isotopic ratios are well known (Altwegg et al. 2015, for example). The isotopic ratio measured in S^+ from comet 1P Halley is in agreement within errors with V-CDT and with the ratios from dust, as are the ratios measured in CS for C/2012 F6 and C/2014 Q2. The ratios in CS from 17P Holmes and the result in from C/1995 O1, although high, agree within errors with the average result of this work. The remaining measurements from gas are uniformly lower than V-CDT or the dust measurements. Some are significantly lower.

The discrepancy between isotopic ratios between the gas and dust of the same comet is potentially explicable by varied chemistry that produces disparate results in different gaseous species or by a process that only or preferentially affects the volatiles, such as photodissociation of H_2S by solar UV (Chakraborty et al. 2013) or photopolymerization of CS_2 (Zmolek et al. 1999). Calmonte (2015) notes the similarity between the range of sulphur isotopic fractionation observed in cometary gas and presolar silicon carbide grains, and suggests a hypothesis in which H_2S ice formed on SiC grains. In this scenario, grain surface chemistry serves to transmit the isotopic fingerprint of the sulphur in the SiC grains to the H_2S then later sublimation of the H_2S ice spreads the effect to other sulphur-bearing molecules in the gas phase. Altwegg et al. (2017) report a high ratio of HDS/H_2S measured using ROSINA and attribute that to the production of cometary H_2S by presolar grain surface chemistry. The role of grain surface chemistry

in producing sulphur-bearing species is also asserted by Calmonte et al. (2016). In these scenarios, at least some volatile ices must have been incorporated in unaltered form into comet 67P. The isotopic composition of the dust (which matches other many other Solar system objects) could then be primordial.

Although Jessica, Kerttu and Andrzej were collected early in the mission (in 2014 and early 2015), Günter was collected much later – in early 2016. While Günter has the highest isotopic ratio, the difference is easily explicable in terms of the uncertainties in the ratios. No temporal variation can be inferred from this data.

6 CONCLUSION

A long (≈48 h) ToF-SIMS measurement with COSIMA found an average value for the $^{34}S/^{32}S$ ratio in four cometary dust particles of 0.0463 ± 0.0057, which agrees within errors with the V-CDT value of 0.0442. It also agrees within errors with the average isotopic ratio measured in dust impact residues taken from craters on the STARDUST aluminium foils and with the ratio measured in a STARDUST terminal particle.

Comparisons with values of the sulphur isotopic ratio in cometary gas are more problematic. The measurements in S^+ from Halley, in CS from 17P Holmes, C/2012 F6 and C/2014 Q2, and in H_2S from C 1995/O1 agree within errors. The value measured in CS from C 1995/O1 is significantly lower. The recent measurements of the sulphur isotopic ratio in five different species (H_2S, SO_2, CS_2, OCS and S_2) using ROSINA are uniformly lower than the value presented here. It is likely that this represents an actual difference in isotopic composition between the gas and the dust. Such a difference may result from grain surface chemistry in the presolar cloud or some other process which preferentially affected volatiles such as photodissociation or photopolymerization. In this case, the isotopic composition of the dust could be the primordial sulphur isotopic composition.

ACKNOWLEDGEMENTS

COSIMA was built by a consortium led by the Max-Planck-Institut für Extraterrestrische Physik, Garching, Germany in collaboration with Laboratoire de Physique et Chimie de l'Environnement et 8 de l'Espace, Orléans, France, Institut d'Astrophysique Spatiale, CNRS/Université Paris Sud, Orsay, France, Finnish Meteorological Institute, Helsinki, Finland, Universität Wuppertal, Wuppertal, Germany, von Hoerner und Sulger GmbH, Schwetzingen, Germany, Universität der Bundeswehr, Neubiberg, Germany, Institut für Physik, Forschungszentrum Seibersdorf, Seibersdorf, Austria, Institut für Weltraumforschung, Österreichische Akademie der Wissenschaften, Graz, Austria and is led by the Max-Planck-Institut für Sonnensystemforschung, Göttingen, Germany. The support of the national funding agencies of Germany (Deutsches Zentrum für Luft-dun Raumfahrt ÜNES, grant 50 QP 1302), France (Centre National d'Études Spatiales), Austria, Finland and the European Space Agency Technical Directorate is gratefully acknowledged. We thank the Rosetta Science Ground Segment at ESAC, the Rosetta Mission Operations Centre at ESOC and the Rosetta Project at ESTEC for their outstanding work enabling the science return of the Rosetta Mission.

REFERENCES

Altwegg K., 1996, Habilitationsschrift. Univ. Bern
Altwegg K. et al., 2015, Science, 347, 1261952
Altwegg K. et al., 2017, Phil. Trans. R. Soc. A, 375, 20160253
Biver N. et al., 2008, LPI Contributions, 1405, 8146
Biver N. et al., 2016, A&A, 589, A78
Bockelée-Morvan D. et al., 2015, Space Sci. Rev., 197, 47
Bullock E. S., McKeegan K. D., Gounelle M., Grady M. M., Russell S., 2010, Meteorit. Planet. Sci., 45, 885
Busemann H., Young A. F., Alexander C. M. O., Hoppe P., Mukhopadhyay S., Nittler L. R., 2006, Science, 312, 727
Calmonte U., 2015, PhD thesis, Univ. Bern
Calmonte U. et al., 2016, MNRAS, 462, S253
Canaves M. V., de Almeida A. A., Boice D. C., Sanzovo G. C., 2007, Adv. Space Res., 39, 451
Chakraborty S., Jackson T. L., Ahmed M., Thiemens M. H., 2013, Proc. Natl. Acad. Sci., 110, 17650
Cooper G. W., Thiemens M. H., Jackson T. L., Chang S., 1997, Science, 277, 1072
Cotter R. J., 1997, Time-of-Flight Mass Spectrometry: Instrumentation and Applications in Biological Research, ACS Professional Reference Books, American Chemical Society, Washington, DC
Crovisier J., Bockelée-Morvan D., Colom P., Biver N., Despois D., Lis D. C., The Team for Target-of-Opportunity Radio Observations of Comets, 2004, A&A, 418, 1141
Defouilloy C., Cartigny P., Assayag N., Moynier F., Barrat J.-A., 2016, Geochim. Cosmochim. Acta, 172, 393
Ding T., Valkiers S., Kipphardt H., De Biévre P., Taylor P. D. P., Gonfiantini R., Krouse R., 2001, Geochim. Cosmochim. Acta, 65, 2433
Farquhar J., Jackson T. L., Thiemens M. H., 2000, Geochim. Cosmochim. Acta, 64, 1819
Floss C., Stadermann F. J., Bradley J. P., Dai Z. R., Bajt S., Graham G., Lea A. S., 2006, Geochim. Cosmochim. Acta, 70, 2371
Fray N. et al., 2016, Nature, 538, 72
Gao X., Thiemens M. H., 1993, Geochim. Cosmochim. Acta, 57, 3159
Gillis N., Vavasis S. A., 2014, IEEE Trans. Pattern Anal. Mach. Intell., 36, 698
Heck P., Hoppe P., Huth J., 2012, Meteorit. Planet. Sci., 47, 649
Hilchenbach M. et al., 2016, Astrophys. J. Lett., 816, L32
Hornung K. et al., 2014, Planet. Space Sci., 103, 309
Jewitt D., Matthews H. E., Owen T., Meier R., 1997, Science, 278, 90
Joswiak D. J., Brownlee D. E., Matrajt G., 2013, Meteorit. Planet. Sci., 48, A194
Kissel J. et al., 2007, Space Sci. Rev., 128, 823
Labidi J., Farquharb J., Alexanderc C.O'.D., Eldridgeb D. L., Odurod H., 2017, Geochim. Cosmochim. Acta, 196, 326
Langevin Y. et al., 2016, Icarus, 271, 76
McKeegan K. D. et al., 2006, Science, 314, 1724
Mumma M. J., Charnley S. B., 2011, Annu. Rev. Astron. Astrophys., 49, 471
Nakamura T. et al., 2008, Science, 321, 1664
Nakashima D., Ushikubo T., Joswiak D. J., Brownlee D. E., Matrajt G., Weisberg M. K., Zolensky M. E., Kita N. T., 2012, Earth Planet. Sci. Lett., 357, 355
Nguyen A. N., Berger E. L., Nakamura-Messenger K., Messenger S., 2015, Meteorit. Planet. Sci., 50, Special Issue: SI Supplement: 1 Meeting Abstract: 5375.pdf
Nittler L. R., Davidson J., Liu N., Alexander C.O'.D., Stroud R. M., 2015, Lunar Planet. Sci. Conf. 46, Abstract #2097
Ogliore R. C. et al., 2012, Astrophys. J. Lett., 745, L19
Paquette J. A., Engrand C., Stenzel O., Hilchenbach M., Kissel J., the COSIMA Team, 2016, Meteorit. Planet. Sci., 51, 1340
Rai V. K., Jackson T. L., Thiemens M. H., 2005, Science, 309, 1062
Rotundi A. et al., 2015, Science, 347, aaa3905
Simon S. B. et al., 2008, Meteorit. Planet. Sci., 43, 1861
Smith A. M., Stecher T. P., Casswell L., 1980, Astrophys. J., 242, 402
Zmolek P., Xu X., Jackson T., Thiemens M. H., Trogler W. C., 1999, Phys. Chem. A, 103, 2477

This paper has been typeset from a Microsoft Word file prepared by the author.